

Prediction of space-time correlations by large eddy simulation

Guo-Wei He^{1,2†}, Hua-dong Yao¹, Xin Zhao¹

¹ LNM, Institute of Mechanics, Chinese Academy of Sciences, Beijing, 100080, P. R. China

² Department of Aerospace Engineering, Iowa State University, Ames, IA 50011-2271

Abstract

The recently increasing application of large eddy simulation to unsteady problems [1], such as turbulence-generated sound and turbulent reacting flows, requires that large-eddy simulation (LES) with a sub-grid scale (SGS) model could accurately predict space-time correlations. Most of the currently existing SGS models are based on the energy budget equations. Therefore, they are able to correctly predict energy spectra at large scales, but they may not accurately predict other statistical quantities that are not determined fully by large-scale energy spectra, such as space-time correlations. In this paper, we will investigate the effects of SGS modeling on space-time correlations in LES. The numerical simulations of isotropic turbulence [2, 3] and turbulence channel flows [4] show that, compared with the results of direct numerical simulation (DNS), LES under-predicts the un-normalized correlation magnitude and over-predict the decorrelation time scales. This can lead to inaccurate solutions in applications such as sound power spectra. In turbulence-generated sound, according to Lighthill's theory, the acoustic intensity radiated by turbulent flows depends on two-point, two-time correlations, or Eulerian space-time correlations. Therefore, an accurate calculation of the Eulerian space-time correlation is important to the prediction of the sound radiations. The application of space-time correlations to acoustic power in LES is also discussed.

1 Introduction

Space-time correlations or their Fourier transformations, wavenumber-frequency spectra, are the simplest but fundamental measurements on turbulent fluctuating in space and time. The statistic quantity has a wide application to turbulent flows in various industries such as aeronautics and aerospace. For example, sound radiated by turbulent flows is dependent on the space-time characteristics of the flow field. According to Lighthill's theory [1, 2], acoustic power spectra in the far-fields are determined by the two-time, two-point Eulerian velocity correlations; In turbulence control and drag reduction [3], the space-time characteristics of turbulent fluctuations are required as control inputs for the blowing and suction of the actuator; The flow-induced vibrations are also dependent on the wavenumber-frequency spectra of turbulent fluctuations [4]. In boundary layer receptivity [5], the wavenumber-frequency spectra of disturbances in the free-stream determine the initial fluctuations entering the boundary layers, which induces the transition from laminar to turbulent flows; In aero-optics [6], the intensive space-time intermittence of turbulent flows may induce a time-varying aberration of planar of a light beam through the flow field. Other applications include heat transfer, particle dispersion and predictability. Therefore, space-time correlations of turbulent fluctuations have significant implications to the use of large eddy simulations for those problems. Therefore, it is natural to ask whether or not the LES with an appropriate SGS model can correctly predict the space-time correlations.

The previous researches [7, 8] compare the space-time correlations evaluated by DNS and LES in isotropic turbulence. The comparison shows that the LES overpredicts decorrelation time

†: The correspondent author. E-mail: hgw@lnm.imech.ac.cn or guoweihe@yahoo.com.

scales and underpredicts the correlation magnitudes. These results have been confirmed by Park et al [9] in isotropic turbulence and Martin [10] in turbulence boundary layers. In this paper, we will investigate the prediction by LES of space-time correlations in turbulent shear flows. In section II, we will review the results on space-time correlations in isotropic turbulence and use those results to study the LES for acoustic power; in section III, we will evaluate the performance of LES on space-time correlations in turbulent channel flows; in section III, we will summarize the results and present the conclusions.

2 Space-time correlations in isotropic turbulence

In this section, we will investigate the prediction by LES of space-time correlations in isotropic turbulence. The space-time correlation can be equivalently expressed by the two-time correlations of velocity Fourier modes in spectral space

$$C(k, \tau) = \langle u_i(\mathbf{k}, t) u_i(-\mathbf{k}, t + \tau) \rangle. \quad (1)$$

This quantity will be calculated from the DNS and compared with the one from the LES. Furthermore, the effects of time correlation errors in LES on acoustics prediction will be examined using Lighthill's analogy. According to the Lighthill analogy ([1]), the acoustic pressure in a far-field position \mathbf{x} is given by

$$p(\mathbf{x}, t) = \frac{1}{4\pi c^2} \frac{x_i x_j}{|\mathbf{x}|^3} \int_{\Omega} dy \frac{\partial^2}{\partial t^2} T_{ij} \left(\mathbf{y}, t - \frac{|\mathbf{x} - \mathbf{y}|}{c} \right), \quad (2)$$

where $T_{ij}(\mathbf{y}, t) = \rho u_i(\mathbf{y}, t) u_j(\mathbf{y}, t)$ is the Lighthill stress tensor, Ω the source region, ρ the mean far-field density, c the speed of sound in the far-field, and \mathbf{y} a position vector in the source field. The sound power spectra can be then calculated as $p(\mathbf{x}, \omega)p(\mathbf{x}, -\omega)$ at the far-field \mathbf{x} .

2.1 The random sweeping model in isotropic turbulence

Kraichnan [11] and Tennekes [12] propose a random sweeping hypothesis for space-time correlations in isotropic turbulence: the dominant effects on space-time patterns at high frequencies is the random sweeping of small eddies by energy-containing eddies. This hypothesis yields a universal form of space-time correlations. Consider a Fourier mode $\mathbf{u}(\mathbf{k}, t)$ of fluctuating velocity convected by a large scale velocity field \mathbf{v} , where \mathbf{v} is a uniform Gaussian field and independent of the fluctuating velocity $\mathbf{u}(\mathbf{k}, t)$. Following the assumption in the random sweeping hypothesis that the viscous effect and nonlinear terms in \mathbf{u} may be neglected in the Navier-Stokes equations, we obtain

$$\frac{\partial \mathbf{u}(\mathbf{k}, t)}{\partial t} + i(\mathbf{k} \cdot \mathbf{v}) \mathbf{u}(\mathbf{k}, t) = 0. \quad (3)$$

The solution of Eq. (3) is

$$\mathbf{u}(\mathbf{k}, t) = \mathbf{u}(\mathbf{k}, 0) \exp[-i(\mathbf{k} \cdot \mathbf{v})t]. \quad (4)$$

Then, the time correlation can be expressed as [7, 11]

$$C_u(k, \tau) = \langle u_i(\mathbf{k}, t) u_i(-\mathbf{k}, t) \rangle \exp\left(-\frac{1}{2} v^2 k^2 \tau^2\right), \quad (5)$$

where the sweeping characteristic velocity $v = |\mathbf{v}|$ is the r.m.s. of velocity fluctuations. The random sweeping hypothesis for fluctuating velocities was verified using the DNS data and has been recently extended to pressure fluctuations. It can be seen from the random sweeping model

(5) that the time correlations are determined by the energy spectra and the sweeping velocity. Since the sweeping velocity is determined by the energy spectra, the accurate prediction of time correlations is determined by the accurate prediction of energy spectra in isotropic turbulence.

2.2 Time correlations of velocity modes: DNS vs LES

We will compare the time correlations from the DNS with the ones from the LES. A decaying homogeneous isotropic turbulence in a cubic box of side 2π is simulated by DNS with grid size 256^3 and LES with grid size 64^3 . The following SGS models are used in the LES: (1) the spectral eddy-viscosity SGS model [13]; (2) The Smagorinsky SGS model [14];(3) The dynamic Smagorinsky SGS model [15]; (4) The multiscale LES method with dynamic SGS model [16].

Fig. 1 plots the space-time correlations of fluctuating velocities from the DNS and LES for wavenumber $k = 5, 9, 13$ and 17 , spanning a range of scales from the integral scale to the lower end of the resolved scales. The starting time is $t = 0.5$. A comparison clearly shows that there exist discrepancies between the LES and DNS results. These discrepancies become larger with increasing wavenumbers. Among the SGS models used here, the classic Smagorinsky model results are the least accurate and the multiscale LES is the most accurate. the dynamic Smagorinsky model and spectral eddy-viscosity model yield comparable results for the comparable results for the first two wavenumbers but the former is significantly more accurate at two higher wavenumbers.

A further investigation using the random sweeping model yields more concrete results: the LES under-predict the space-time correlations of the DNS in magnitude and over-predict their decorrelation length scales in time. The reason for the time correlation errors in LES can be understand as follows: The LES under-predict the magnitudes of time correlations because the energy spectrum levels are lower in LES than the one in DNS, and over-predicts the decorrelation time scales because the sweeping velocity in LES is smaller than the one in DNS.

2.3 Sound power spectra: DNS vs LES

We are now use the DNS data to test the Lilley model [17] for sound power level (SPL) of the radiated noise from isotropic turbulence and use the LES data to study the prediction of the SPL by LES. The DNS for isotropic turbulence was performed using a pseudo-spectral method. The computational domain is a box of length 2π on each side, where the periodic boundary conditions are applied. To keep the turbulence stationary, an external force $f(k)$ is imposed on the first two shells of wavenumbers $k = 1, 2$. Aliasing errors are removed through the two-thirds truncation rule. The Adams-Bashforth scheme is used for time advance. Three cases for DNS are run in the present study: Case 1 with $\text{Re}_\lambda = 78.75$ on a 128^3 grid, Case 2 with $\text{Re}_\lambda = 148.92$ on a 256^3 grid and Case 3 with $\text{Re}_\lambda = 206.58$ on a 512^3 grid, respectively. Two cases for LES are run in comparison with Case 3 of the largest Re: Case 4 on a 256^3 grid and Case 5 on a 128^3 grid, using the spectral eddy-viscosity SGS model. The relevant parameters in the DNS and LES are listed in Table 1.

Fig. 2 compares the SPLs from the DNS at Case 1, 2 and 3 with the Lilley model. It can be seen from the figure that the DNS results at higher Re are in better agreement with the Lilley model. We also use the present DNS data to test other SPL models and find that the Lilley model is the best one to fit the DNS data at the largest Re.

In Fig. 3(a), the sound power spectra (SPS) computed from the resolved Lighthill tensor are plotted as the functions of St using the DNS and LES data. Overall, the LES results are consistent with the DNS one. However, the peaks of the SPS in LES are located at the left-hand-side of the one in DNS. More Surprisingly, their amplitudes are larger than the one in DNS at small strouhal number while they are smaller than the one in DNS at large St. The reason for it can be understand as follows: the LES under-predicts the sweeping velocity, which yields a different weight function to the energy spectra in the Lighthill formulism.

Fig. 3(b) plots the sound power level (SPL) as a function of the strouhal number for DNS and LES. It is clearly observed that the SPLs in LES drop faster than the one in DNS at high St, with the LES 256^3 result being between the LES 128^3 and DNS 512^3 results. Therefore, the LES under-predict the SPL at high St rather than the DNS.

3 Space-time correlations in turbulent shear flows

3.1 The elliptic model in turbulent shear flows

The turbulence space-time correlations theory suggests that the dominant effects on space-time patterns at high frequencies is the sweeping of small eddies pass a fixed point by large eddies. This implies that the space-time fluctuations can be expressed as an appropriate transformation of space correlations. Taylor frozen flow hypothesis [18] assumes that the transformation is linear such that

$$R(r, \tau) = R(r - U\tau, 0). \quad (6)$$

The linear transformation implies that the iso-correlation contours are straight lines: $r - U\tau = C$ with C being a contour level. However, Taylor's hypothesis has many limitations such as weak shear rate and low turbulence intensity. It is not accurate for turbulent shear flows. Therefore, we propose a second approximation to the iso-correlation contours and develop a contour similarity model for space-time correlations in turbulent shear flows. The elliptic model [19] suggests that the space-time correlation are determined by the space correlations and two characteristic velocities, such that

$$R(r, \tau) = R\left(\sqrt{(r - U\tau)^2 + (V\tau)^2}, 0\right), \quad (7)$$

where U is a convection velocity and V a sweeping velocity. The former represents the propagation of velocity fluctuations and the latter represents the decorrelation of velocity fluctuations themselves. In homogeneous turbulent shear flows, the two characteristic velocities are

$$U = U_1, \quad (8)$$

$$V^2 = (S\lambda)^2 + \langle v_i^2 \rangle, \quad (9)$$

where U_1 , is the mean velocity, S the shear rate, λ the Taylor microscale and v_i the fluctuating velocities. The convection velocity is the mean velocity and the sweeping velocity is the sum of the shear-induced velocity and r.m.s of fluctuating velocity.

3.2 Space-time correlations: DNS vs LES

The direct numerical simulation (DNS) of turbulent channel flows is performed and used to study the prediction by LES of space-time correlations in turbulent shear flows. The necessary parameters for DNS are as follows: $Re_\tau = 180$ and the grid resolution is $128 \times 129 \times 128$.

Fig. 4 plots the iso-correlation contours of fluctuating velocities in the streamwise direction at $y^+ = 2.4$ (viscous sublayer), where the contour levels are typically 0.9 and 0.6. Fig. 4(a) compares the contours obtained from DNS with the ones from the filtered DNS and Fig. 4(b) compares the DNS results with the LES ones. It is observed from them that the contours from LES are larger than the ones from DNS in size while the contours from the filtered LES are approximately equal the ones from DNS. These observations imply that the correlations from the LES decay slower than the ones from DNS while the correlations from the filtered DNS decay at the almost same rates as the ones from DNS. Therefore, the SGS modeling has significant effects on the space-time correlations.

Fig. 5 shows the correlation lines for those space and time separations that are located in the major axis of the iso-correlation contours. The correlations $R(r, \tau)$ are plotted against the separation magnitude $\sqrt{r^2 + \tau^2}$ for $r = \tau \tan(\alpha)$, where $\tan(\alpha)$ is the slope of the preferred orientation. It is observed that the correlation lines from LES decay much slower than the ones from DNS while the decay rate of the correlations from the filtered DNS are comparable with the ones from the DNS. Those observations are consistent with the previous ones on the iso-correlation contours. We also plot in Fig. 6 the correlation lines in the direction of the minor axis. The results for the minor axis are qualitatively same as the ones for the major axis. However, the differences between the LES and DNS results for minor axis are larger than the ones for major axis. Therefore, Figures 5 and 6 show that the LES significantly over-predicts the space-time correlations in DNS.

We compare the iso-correlation contours in Fig. 7 and the correlation functions in Figures 8 and 9 for DNS, the filtered DNS and LES at $y^+ = 91.9$ (log-law regime). The comparisons indicate that the LES results evidently deviate from the DNS results while the filtered LES results are approximately equal to the LES results. Those results are consistent with the ones at $y^+ = 2.4$. However, the differences between LES and DNS are smaller at $y^+ = 91.9$ than the ones at $y^+ = 2.4$. This implies that the LES prediction of space-time correlations are better at weak shear rates.

The overprediction of the space-time correlations by LES than DNS can be understood using the elliptic model. In LES, the convection velocity U , mean shear rate S and the total energy $\langle v_i^2 \rangle$ of fluctuating velocities can be correctly calculated. However, the Taylor length microscales are over-estimated by LES. Therefore, the separation $(r - U\tau)^2 + (V\tau)^2$ in LES is larger than the one in DNS. Thus, the correlation decay more slowly in LES than in DNS. In fact, suppose that k_c is the filter wavenumber, we can compare the energy and enstrophy in DNS and LES

$$\begin{aligned} \int_0^\infty E(q) dq &= \int_0^{k_c} E(q) dq \\ \int_0^\infty q^2 E(q) dq &\geq \int_0^{k_c} q^2 E(q) dq \end{aligned} \quad (10)$$

The LES can approximately predict the total energy of DNS but under-estimate the enstrophy of DNS and thus, it overpredicts the Taylor length microscales. Therefore, enstrophy is critical to the LES prediction of space-time correlations.

4 Conclusions and discussions

Numerical simulations in both isotropic turbulence and turbulent channel flows show that there exist discrepancies in space-time correlations evaluated by DNS and LES. In isotropic turbulence, LES predicts smaller magnitudes of the correlations than the DNS does but larger decorrelation time scales than the DNS does. In turbulent channel flows, the same observations are obtained where the LES over-predicts the decorrelation time scales rather the DNS. The overpredictions are significant especially at the regions of strong shear rates. The overpredictions decrease as the shear rates become smaller. The space-time correlation errors in LES leads that the SPL in LES deviates from the one in DNS: the peak of SPL in LES is off the one in DNS to the left, with the underprediction at larger St and overprediction at small St.

The analysis based on the space-time correlation models explains the discrepancies in our numerical simulations. In isotropic turbulence, the magnitude of space-time correlations are mainly determined by energy spectra and the decorrelation time scales mainly determined by sweeping velocity. Since the energy spectra evaluated by LES is lower than the ones in DNS and thus the sweeping velocity in LES is smaller than the one in DNS, the LES under-predicts the magnitude of space-time correlations and over-predict the decorrelation time scales in DNS. Therefore, in isotropic turbulence, an accurate prediction of energy spectra is critical to the accurate prediction of space-time correlations by LES. In turbulent channel flows, the decorrelation time scales are mainly determined by the mean velocity, the r.m.s of fluctuating velocities, the shear rate and Taylor length time microscale. Since a LES predicts a larger Taylor length time microscale, it over-predicts the decorrelation time scales. Therefore, in turbulent shear flows, the accurate prediction of enstrophy is critical to the accurate prediction of space-time correlation in addition to energy spectra.

ACKNOWLEDGMENTS: This work was supported by Chinese Academy of Sciences under the Innovative Project “Multi-scale modeling and simulation in complex systems” (KJCX-SW-L08), National Basic Research Program of China (973 Program) under Project No. 2007CB814800 and National Natural Science Foundation of China under Project Nos. 10325211, 10628206 and 10732090.

References:

- [1] M. J. Lighthill, “On sound generated aerodynamically: I. General theory,” Proc. R. Soc. London, Ser. A **211**, 564 (1952).
- [2] I. Proudman, “The generation of sound by isotropic turbulence,” Proc. R. Soc. London, Ser A **214**, 119 (1952).
- [3] J. Lumley and P. Blossey, “Control of turbulence,” Annu. Rev. Fluid Mech. **30**, 311 (1998).
- [4] C. H. K. Williamson and R. Govardhan, “Vortex-induced vibrations,” Annu. Rev. Fluid Mech. **36**, 413 (2004).
- [5] W. S. Saric, H. L. Reed and E. J. Kerschen, “Boundary-layer receptivity to freestream disturbance,” Annu. Rev. Fluid Mech. **34**, 291 (2002).
- [6] E. J. Jumper and E. J. Fitzgerald, “Recent advances in aero-optics,” Progress in Aerospace Sciences **37**, 299 (2001).
- [7] G.-W. He, R. Rubinstein and L. P. Wang, “Effects of subgrid-scale modeling on time correlations in large eddy simulation,” Phys. Fluids **14**, 2186 (2002).

- [8] G.-W. He, M. Wang and S. K. Lele, "On the computation of space-time correlations by large-eddy simulation," *Phys. Fluids* **16**, 3859 (2004).
- [9] N. Park, J. Y. Yoo and H. Choi, "Toward improved consistency of a priori tests with a posteriori tests in large eddy simulation," *Phys. Fluids* **17**, 015103 (2005).
- [10] M. P. Martin, "Preliminary study of the SGS time scales for compressible boundary layers using DNS data," AIAA paper No.2005-665, 2005.
- [11] R. H. Kraichnan, "Kolmogorov's hypotheses and Eulerian turbulence theory," *Phys. Fluids* **7**, 1723 (1964).
- [12] H. Tennekes, "Eulerian and Lagrangian time microscales in isotropic turbulence," *J. Fluid. Mech.* **67**, 561 (1975).
- [13] J. P. Chollet and M. Lesieur, "Parametrization of small scales of three-dimensional isotropic turbulence utilizing spectral closure," *J. Atmos. Sci.* **38**, 2747 (1981).
- [14] J. Smagorinsky, "Gerneral circulation experiments with the primitive equations: I. The basic experiment," *Mon. Weather Rev.* **91**, 99 (1963).
- [15] M. Germano, U. Piomelli, P. Moin and W. H. Cabot, "A dynamic subgrid-scale eddy viscosity model," *Phys. Fluids A* **3**, 1760 (1991).
- [16] T. J. R. Hughes, L. Mazzei and A. S. Oberai, "The multiscale formulation of large-eddy simulation: Decay of homogeneous isotropic turbulence," *Phys. Fluids* **13**, 505 (2001).
- [17] G. M. Lilley, "The radiated noise from isotropic turbulence," *Theor. Comput. Fluid Dyn.* **6**, 281 (1994).
- [18] G. I. Taylor, "The Spectrum of turbulence," *Proc. Roy. Soc. A* **164**, 476 (1938).
- [19] G.-W. He and J.-B. Zhang, "Elliptic model for space-time correlations in turbulent shear flows," *Phys. Rev. E* **73**, 055303 (2006).

Table 1: Relevant parameters and statistical quantities in DNS and LES*.

Case	Nodes	Δt	u_{rms}	L	CFL	λ	ξ	Re_λ
Case 1	128^3	0.002	0.843	1.597	0.194	0.599	1.445	78.75
Case 2	256^3	0.001	0.864	1.471	0.267	0.341	1.207	148.92
Case 3	512^3	0.00045	0.871	1.469	0.208	0.238	1.432	206.58
Case 4	256^3	0.0009	0.867	1.476	0.209	--	--	--
Case 5	128^3	0.0018	0.856	1.490	0.210	--	--	--

* Here L is the integral length scale, λ is the Taylor microscale, $\xi = k_{\max} \eta$ indicates the spatial resolution, CFL is the CFL number and Re_λ is the Taylor-scale Reynolds number.

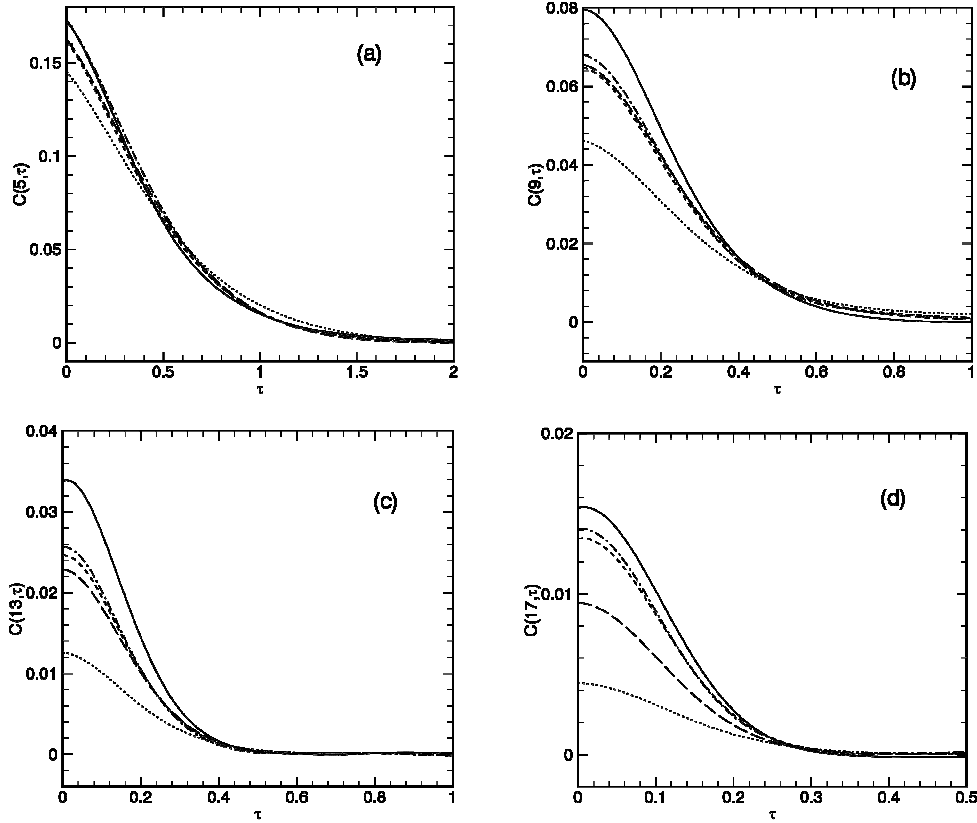


Figure 1. Space-time correlations $C(k, \tau)$ vs time lag τ with starting time $t = 0.5$ for (a) $k = 5$, (b) $k = 9$, (c) $k = 13$, (d) $k = 17$. Solid line: DNS; dashed line: dynamic Smagorinsky model; solid-dotted-line: multiscale LES; dotted line: Smagorinsky model; spectral eddy viscosity model.

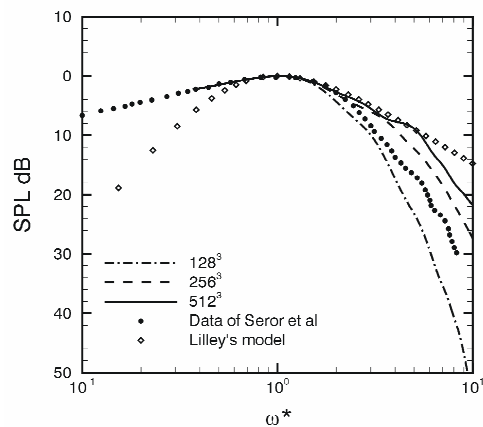


Figure 2. Sound power levels computed from the DNS and the Lilley model.

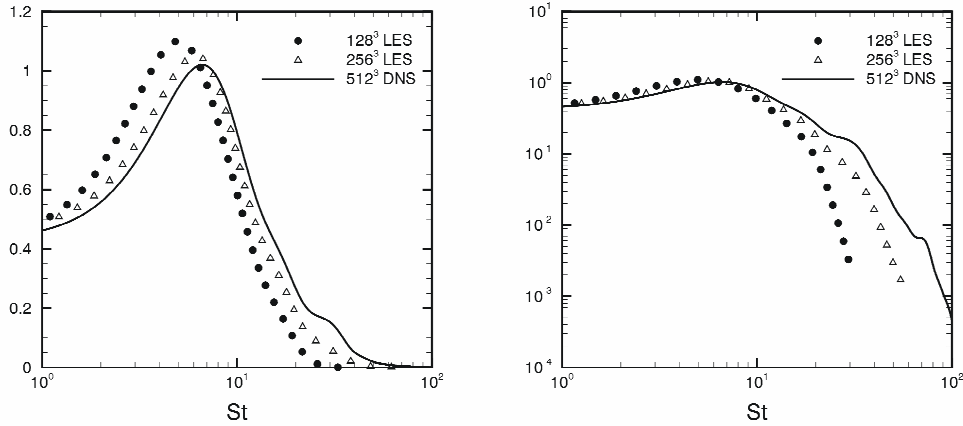


Figure 3. (a) Comparison between sound power spectra computed from DNS and LES; (b) Comparison between sound power level computed from the DNS and LES}.

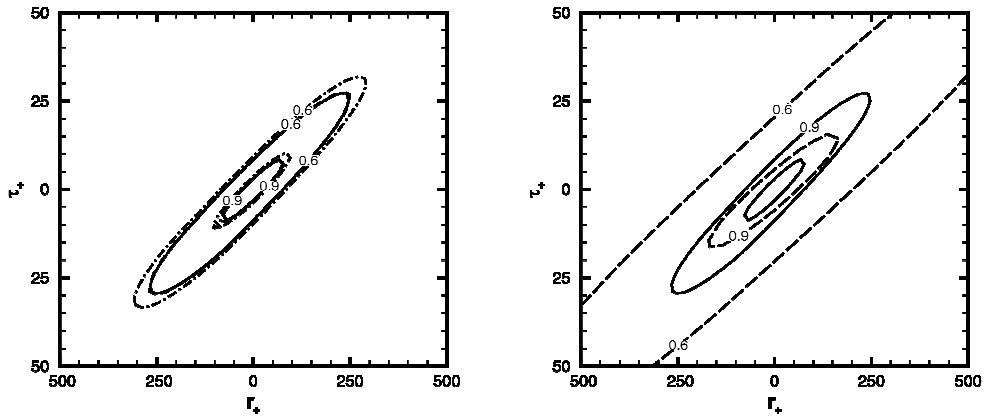


Figure 4. The iso-correlation contours as the functions of space separation and time delay at $y^+ = 2.4$ (viscous sublayer). (a) DNS vs. the filtered DNS: the solid line for the DNS results; the dash line for the filtered DNS results using the filter width $2h$; the dash-dotted line for the filtered DNS results using filter width $4h$. (b) DNS vs. LES: the solid line for the DNS results and the dash line for the LES results.

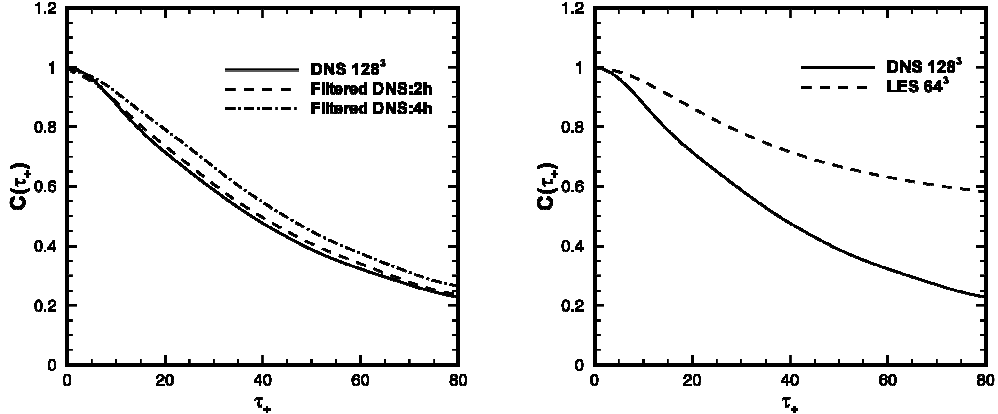


Figure 5. The space-time correlations on the major axis of the iso-correlation contours at $y^+ = 2.4$ (viscous sublayer). (a) DNS vs. the filtered DNS: the solid line for the DNS results; the dash line for the filtered DNS results using the filter width $2h$; the dash-dotted line for the filtered DNS results using filter width $4h$. (b) DNS vs. LES: the solid line for the DNS results and the dash line for the LES results.

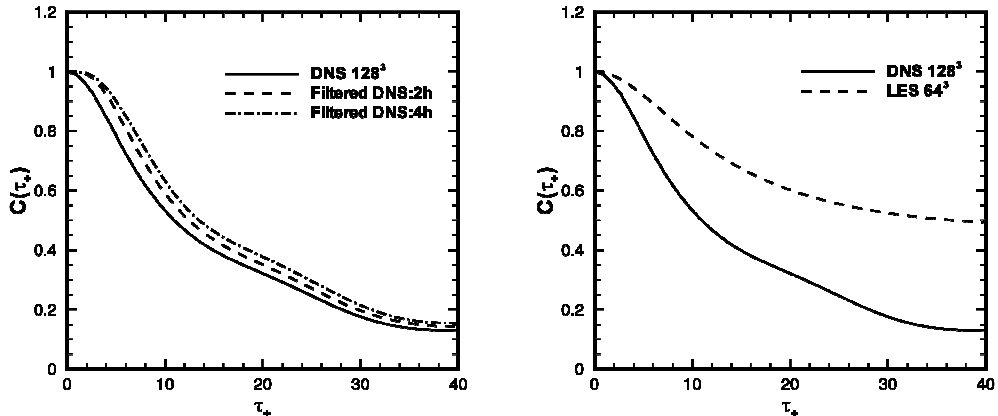


Figure 6. The space-time correlations on the minor axis of the iso-correlation contours at $y^+ = 2.4$ (viscous sublayer). (a) DNS vs. the filtered DNS: the solid line for the DNS results; the dash line for the filtered DNS results using the filter width $2h$; the dash-dotted line for the filtered DNS results using filter width $4h$. (b) DNS vs. LES: the solid line for the DNS results and the dash line for the LES results.

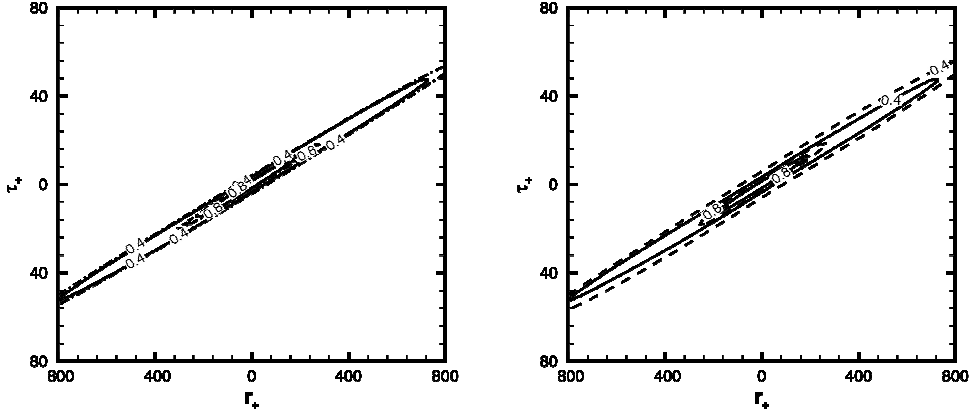


Figure 7. The iso-correlation contours as the functions of space separation and time delay at $y^+ = 91.9$ (log-law region). (a) DNS vs. the filtered DNS: the solid line for the DNS results; the dash line for the filtered DNS results using the filter width $2h$; the dash-dotted line for the filtered DNS results using filter width $4h$. (b) DNS vs. LES: the solid line for the DNS results and the dash line for the LES results.

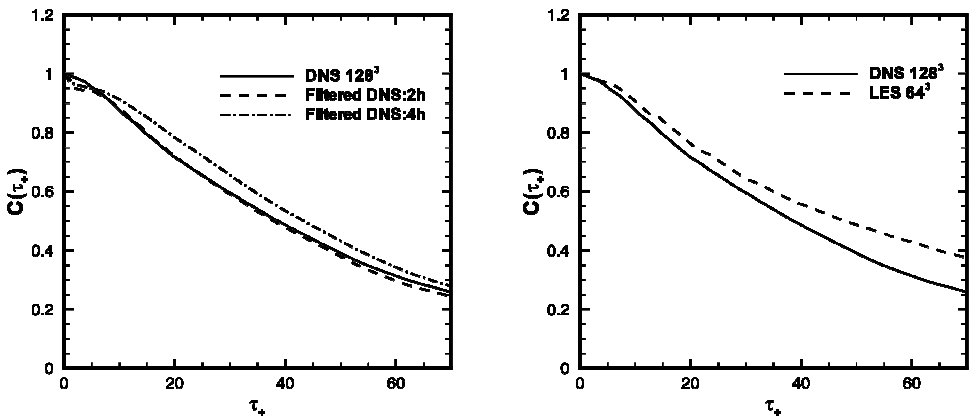


Figure 8. The space-time correlations on the major axis of the iso-correlation contours as functions of time delay at $y^+ = 91.9$ (log-law region). (a) DNS vs. the filtered DNS: the solid line for the DNS results; the dash line for the filtered DNS results using the filter width $2h$; the dash-dotted line for the filtered DNS results using filter width $4h$. (b) DNS vs. LES: the solid line for the DNS results and the dash line for the LES results.

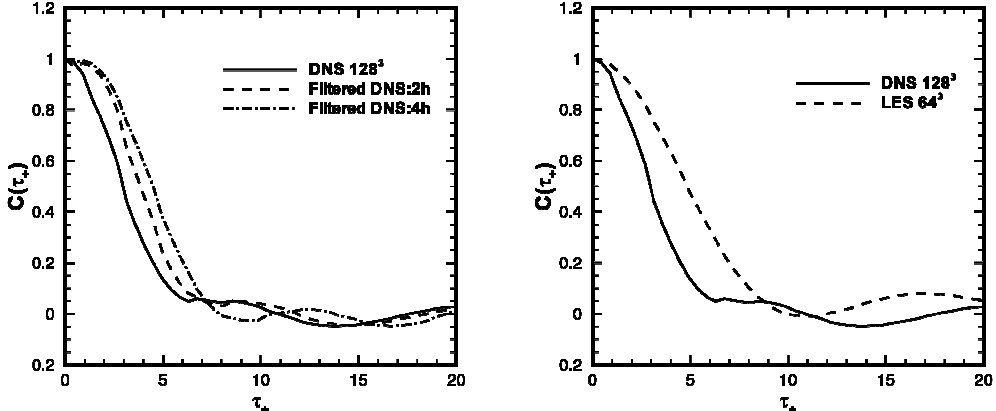


Figure 9. The space-time correlations on the minor axis of the iso-correlation contours as functions of time delay at $y^+ = 91.9$ (log-law region). (a) DNS vs. the filtered DNS: the solid line for the DNS results; the dash line for the filtered DNS results using the filter width $2h$; the dash-dotted line for the filtered DNS results using filter width $4h$. (b) DNS vs. LES: the solid line for the DNS results and the dash line for the LES results.